A Global Analysis of Stratospheric–Tropospheric Exchange during Northern Winter

MARTIN P. HOERLING

Cooperative Institute for Research in the Environmental Sciences, University of Colorado, Boulder, Colorado

TODD K. SCHAACK AND ALLEN J. LENZEN

University of Wisconsin–Madison, Space Science and Engineering Center, Madison, Wisconsin

(Manuscript received 17 December 1991, in final form 27 May 1992)

ABSTRACT

Using a mathematical formulation of stratospheric–tropospheric (ST) exchange, the cross-tropopause mass flux is diagnosed globally for January 1979. Contributions by physical mechanisms including the diabatic transport and the quasi-horizontal adiabatic transport along isentropes that intersect the tropopause surface are evaluated. Both thermal and dynamical definitions of the tropopause are used.

Two regions of zonally integrated mass flux into the stratosphere are found, one over tropical latitudes associated with diabatic transports, and a second over subpolar latitudes associated with adiabatic transports. The ingress to the stratosphere in each of the latitude bands 50°–70°N and 40°–70°S is as intense as that occurring over the tropics, a feature of the global budget not previously documented. Compensating mass outflow from the stratosphere occurs mainly over midlatitudes near axes of strong upper-level westerlies.

Large zonal asymmetries are found in the regional patterns of ST exchange. Consistent with the concept of a stratospheric fountain, the tropical inflow to the stratosphere is maximized over the Australasian monsoon. The midlatitude mass outflow tends to be concentrated along stationary wave troughs, roughly in the vicinity of cyclogenetic areas. A mass transport into the stratosphere occurs downstream and poleward of the troughs. The extratropical pattern of time-averaged cross-tropopause mass flux thus appears to be interpretable within the framework of simple physical models on three-dimensional airmass trajectories in baroclinic disturbances.

While uncertainties concerning quantitative aspects of the global ST exchange remain, qualitative confirmation of the mass-transport diagnostics is found in independent studies of trace atmospheric constituents. In particular, the finding of mass inflow to the stratosphere at subpolar latitudes is consistent with satellite and aircraft measurements of high water vapor mixing ratios in the low stratosphere over these regions.

1. Introduction

Our understanding of global stratospheric–tropospheric (ST) exchange is incomplete, being based largely on regional phenomenological studies (e.g., Reed and Danielsen 1959; Staley 1962; Danielsen 1964, 1968; Reiter et al. 1969; Shapiro 1980; Kritz et al. 1991). Much of our current knowledge of the global budget is derived from Reiter (1975), who attempted to assimilate the findings from case studies with larger-scale analyses of the zonally averaged mass circulation. According to his results for annual-mean conditions, the Hadley cell appears to be the primary mechanism for transporting mass into the stratosphere. Compensating mass flux into the troposphere is believed to occur over middle and high latitudes where the extrusion of stratospheric air in the vicinity of large-scale eddies has been well documented. Considerable uncertainty, however, remains regarding the role played by individual physical processes. For example, the downward exchange in midlatitudes has been inferred from an index of cyclone activity (Mahlman 1964). Presumably, cross-tropopause mass flux also occurs in noncyclogenetic environments associated with the transverse circulations around subtropical jets (Krishnamurti 1961). Additionally, the extent to which mass is returned to the stratosphere by cyclone-scale circulations is unclear.

Little is known about the regional pattern of the time-mean ST exchange, aside from the evidence of a "stratospheric fountain" over the tropical monsoons (Newell and Gould-Stewart 1981). Danielsen (1968) presented empirical evidence for the cross-tropopause mass exchange in midlatitudes associated with upper-level jets. The net ST mass exchange associated with the climatological jets, however, has not been determined.

The purpose of the current study is to diagnose the global and regional distributions of the time-averaged ST mass exchange. The roles of individual processes are examined, including the transport by the Hadley circulation and the transports in extratropics in the

Corresponding author address: Dr. Martin P. Hoerling, Cooperative Institute for Research in the Environmental Sciences, University of Colorado, Boulder, CO 80309.

vicinity of the westerly jets and the storm tracks. Our analysis is based on a model-assimilated dataset that depicts the four-dimensional structure of wind and temperature fields globally. The advantage for investigation of ST exchange is obvious since the homogeneous spatial and temporal sampling of information ensures a self-consistent global analysis. This overcomes a source of uncertainty in previous global estimates that were based on a combination of results from disparate regional studies employing different data sources (Reiter 1975). A disadvantage results from the condition that current global datasets have coarse resolution in both horizontal and vertical dimensions.

Stratospheric–tropospheric mass exchange is diagnosed following the mathematical formulation of Wei (1987). As discussed further in section 2, Wei's model permits a quantification of the flux of any constituent (e.g., mass, water vapor, ozone, etc.) across an arbitrary parametric surface. Furthermore, the contribution to the net flux by individual physical mechanisms can be evaluated. This approach contrasts with previous studies of ST exchange in which numerical estimates were not based on an explicit mathematical formulation. In common with previous studies, however, is the need to define an appropriate tropopause surface that either synoptically or statistically separates the troposphere from the stratosphere.

The difficulties in tropopause analysis are well known (Danielsen 1959; Reiter et al. 1969; Reiter 1975; Danielsen and Hipskind 1980; Hoerling et al. 1991). Various tropopause definitions have been used, including the conventional thermal definition based on lapse-rate criteria and a dynamical definition based on a potential-vorticity (PV) threshold. Recently Hoerling et al. (1991) (hereafter HSL) applied both definitions in analysis of the global tropopause during January 1979 using the European Centre for Medium-Range Weather Forecasts (ECMWF) assimilated dataset. Their results demonstrate an ability to define the large-scale features of the tropopause globally without resort to detailed sounding analysis, and suggest the feasibility of diagnosing ST exchange globally. An important caveat, however, is that although tropopause analyses based on both definitions shown in HSL agree qualitatively with each other, regional differences approach 50 mb. Reiter et al. (1969) show that the mass in a 50-mb layer extending over an area of 350 km × 350 km is equivalent to 24% of the ST exchange in a particular extratropical cyclone. Since it is not known which method yields the best tropopause analysis a priori, ST mass exchange will be diagnosed with respect to both surfaces, thereby providing a measure of uncertainty.

Section 2 contains a description of the diagnostic model used herein for the evaluation of ST mass exchange. Included also are a description of the dataset and the methods of analysis. The temporally and zonally integrated cross-tropopause mass exchange for January 1979 is presented in section 3, while the regional time-mean distributions are described in section 4. Concluding remarks appear in section 5.

2. Methodology

a. *Mathematical formulation of ST exchange*

The cross-tropopause mass transport $F(\rho)$ is given by Eq. (18) of Wei (1987)

$$F(\rho) = \rho J_\theta \underbrace{\left(\frac{d\theta}{dt} \right)}_{(a)} - \underbrace{\frac{\partial \theta}{\partial t_{Z_0}}}_{(b)} - \underbrace{\mathbf{V} \cdot \nabla_{Z_0} \theta}_{(c)} , \tag{1}$$

where Z_0 denotes the tropopause surface, θ is potential temperature, and the hydrostatic isentropic mass density is

$$\rho J_\theta = -\frac{1}{g} \frac{\partial p}{\partial \theta} . \tag{2}$$

Note that the horizontal gradient operator is evaluated along the tropopause surface. Thus, if Z_0 denotes a threshold value of potential vorticity, $\nabla_{Z_0} \theta$ denotes the potential-temperature gradient along a constant PV surface.

According to (1), the cross-tropopause mass flux is determined residually from the imbalance of three processes. Each of these can be identified with distinct physical mechanisms of ST exchange. Term (a) reveals the role of diabatic heating at the tropopause, term (b) expresses the role of tropopause potential-temperature fluctuations including contributions from daily to seasonal shifts in the tropopause position, and term (c) expresses the role of quasi-horizontal exchange due to the mass transport ($\rho J_\theta \mathbf{V}$) along isentropes that intersect the tropopause. The first two terms are identically zero for adiabatic, steady-state conditions. Mass transport $F(\rho)$ is then determined entirely by the adiabatic transport of mass along isentropic surfaces.

Stratospheric–tropospheric exchange diagnosed from (1) is an Eulerian approach that attempts to reconstruct the Lagrangian history of air-parcel displacements in the vicinity of the tropopause. This is to be contrasted with previous estimates based on trajectory analyses (e.g., Danielsen 1964; Reiter et al. 1969). In principle, the two methods are equivalent as shown below for the case where the tropopause is defined as a constant PV surface.

The material derivative of potential temperature in an (x, y, Q, t) framework, where Q denotes a constant-PV surface, is given by

$$\frac{d\theta}{dt} = \frac{\partial \theta}{\partial t_Q} + \mathbf{V} \cdot \nabla_Q \theta + \dot{Q} \frac{\partial \theta}{\partial Q} . \tag{3}$$

A multiplication by ρJ_θ and combination with (1) yields the following equivalent expression for the cross-tropopause mass flux

$$F(\rho) = \rho J_Q \dot{Q}, \tag{4}$$

where the Lagrangian source/sink $\dot{Q}$ represents the "vertical motion" with respect to a constant PV surface, and $\rho J_Q = -g^{-1}\partial p/\partial Q$ is the hydrostatic mass density per incremental (x, y, Q) volume element. Motion across the PV-defined tropopause requires air parcels to gain or lose potential vorticity. One method to diagnose the associated ST exchange is to determine the PV destruction or generation along an air parcel's trajectory (Reed 1955; Staley 1960; Shapiro 1980). A second method, which is used in the current study, involves a local evaluation of $F(\rho)$ employing (1). The sum of terms (a)–(c) residually determines the mass transport across the tropopause due to PV sources and sinks given by (4).

b. *Tropopause analysis*

For reasons discussed in the Introduction, two definitions of the tropopause will be used for evaluating ST exchange. Following the World Meteorological Organization (WMO), a thermal method is used that defines the tropopause as the lower boundary of a layer in which the temperature lapse rate is less than 2°C km^{-1} for a depth of at least 2 km. A dynamical definition based on potential vorticity is also used. Hoerling et al. examined the sensitivity of tropopause analyses employing various PV thresholds. It was found that the PV value 3.5×10^{-6} K m^2 kg^{-1} s^{-1} (to be subsequently referred to as 3.5 PV units) represents an optimal value for tropopause analysis in extratropics using the January 1979 ECMWF assimilated data. We adopt a 3.5 PV threshold for analysis of global ST exchange.

The reader is referred to HSL for a detailed discussion on the methodology used to evaluate the tropopause level. The thermally defined tropopause is determined globally. In contrast, the dynamically defined tropopause is only well defined outside the tropics. The dynamical method fails in the tropics since PV vanishes near the equator. We thus produce a "blended" analysis that uses the dynamical definition poleward of 28° latitude and the thermal definition equatorward of 13° latitude. The analysis in subtropics is based on a weighted average of dynamically and thermally derived tropopause pressures according to

$$P = (W)P_{\text{dynamical}} + (1 - W)P_{\text{thermal}}, \tag{5}$$

where the weights W are defined by

$$W = A\,\text{sech}(\phi) + B\phi^2 + C. \tag{6}$$

The coefficients in (6) are empirically derived such that $W = 1$ at $\phi = 28°$ and $W = 0$ at $\phi = 13°$. As shown in Fig. 1, W is a smooth curve with equal weights at $\phi = 22°$. The resultant tropopause surface is guaranteed to be a continuous function of latitude, thereby permitting a proper evaluation of the cross-tropopause flux.

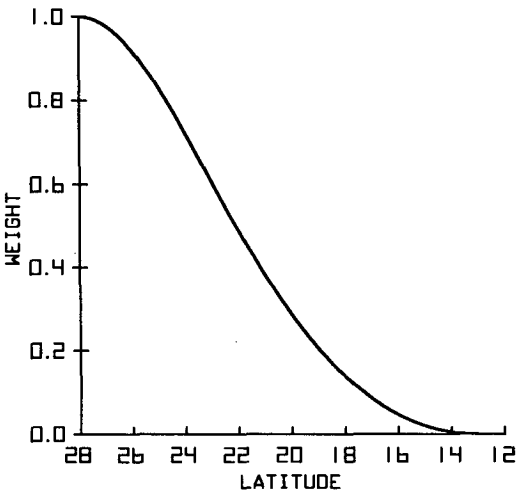

FIG. 1. Weighting function W used to determine pressure on the dynamical tropopause between 28° and 13° latitude.

c. *Dataset*

The data used are from the twice-daily (0000 and 1200 UTC) ECMWF Global Weather Experiment (GWE) final level IIIb uninitialized analyses for January 1979. The isobaric data are available on 15 mandatory pressure levels between 1000 and 10 mb. For analysis of ST exchange, the isobaric data are interpolated to isentropic surfaces at 5-K vertical resolution between 220 and 400 K, and 10-K vertical resolution between 400 and 460 K (see HSL for details). The horizontal resolution of the data used herein is 3.75° latitude × 3.75° longitude. We have also evaluated (1) using 1.875° × 1.875° data. For the large spatial scales emphasized herein, the results are found not to be appreciably different from those derived using the 3.75° data.

The evaluation of the cross-tropopause mass flux in (1) requires specification of the basic meteorological parameters of zonal wind u, meridional wind v, potential temperature θ, and the derived parameters of ρJ_θ and $\rho J_\theta \dot{\theta}$ on the tropopause surface. The hydrostatic isentropic mass density ρJ_θ is calculated on isentropic levels. The diabatic mass flux $\rho J_\theta \dot{\theta}$ is computed on isentropic levels by vertically integrating the isentropic continuity equation (Johnson 1980) with an upper-boundary constraint that $\rho J_\theta \dot{\theta} = 0$ at 460 K. A complete description of the numerical procedure used to calculate the diabatic mass flux is found in Schaack et al. (1990).

Following HSL, at individual grid points the thermally defined tropopause is required to occur at an isentropic data level corresponding to the lower-valued isentropic level bounding the layer for which the WMO lapse-rate criteria are satisfied. In this case, the values of the aforementioned basic and derived parameters are taken directly from the isentropic data. The dynamically defined tropopause is assigned to the vertical

position where the potential vorticity first exceeds 3.5 PV units, and thus may occur between isentropic data levels (see section 2b of HSL). In this case, the aforementioned parameters are interpolated from θ levels to the tropopause surface assuming a linear variation with p^{κ} ($\kappa = R/c_p$). Following the specification of the above parameters on the tropopause surface, terms (b) and (c) in (1) are evaluated on the tropopause surface. The analyses are performed on both thermally and dynamically defined tropopause surfaces twice daily at 0000 and 1200 UTC during January 1979, and subsequently time averaged.

The regional distributions of ST exchange shown in section 4 have been spatially filtered in order to emphasize the large-scale features. First, zonal harmonics having wavelengths less than 6000 km are truncated. Spatial smoothing is employed meridionally using four passes of a low-pass (2, 3, 2) filter and one pass of an inverse (−1, 5, −1) filter, following Schaack et al. (1990).

3. The zonally integrated ST exchange

Figure 2 illustrates the meridional structure of the temporally and zonally averaged tropopause surface for January 1979. Maximum tropopause potential temperatures (Fig. 2a) are 385 K ($T \approx -70$°C) in subtropical latitudes, while minimum values approach 310 K ($T \approx -50$°C) over the Northern Hemisphere (NH) pole. Large meridional variations are concentrated in midlatitudes with the strongest gradient located in the NH, consistent with the greater intensity of the boreal winter circulation. The associated pressure topography verifies the steep slope of the time-mean subtropical tropopause (Fig. 2b) with the pressure increasing from 100 mb at 25°N to 250 mb near 45°N. The isentropic mass density on the tropopause exhibits a similar meridional structure (Fig. 2c).

Both tropopause definitions lead to similar meridional structures, although the thermally defined tropopause is slightly steeper in midlatitudes. Overall, the results in Figs. 2a and 2b are consistent with the tropopause inferred from Danielsen's (1984) zonal- and annual-mean distributions of θ and PV for an 8-yr climatology. It is evident from these analyses that averaging over longitude and time acts to heavily filter the undulations of the tropopause surface. Note in Fig. 2 that only a single discontinuity separating tropical and polar air is distinguishable in each hemisphere. This smoothed *statistical* tropopause is to be contrasted with the more detailed structure of the *synoptic* tropopause. Meridional cross sections along a particular longitude for synoptic time periods may contain a multifold structure (Defant and Taba 1957; Palmen and Newton 1969; Shapiro et al. 1987) in contrast to the simple pattern seen in Fig. 2. In this regard, we should emphasize that the analyses of ST exchange discussed hereafter are derived from twice-daily evaluations performed with respect to the synoptic tropopause. The cross-tropopause mass flux evaluated with respect to the statistical tropopause would likely render a significantly different estimate of the ST exchange.

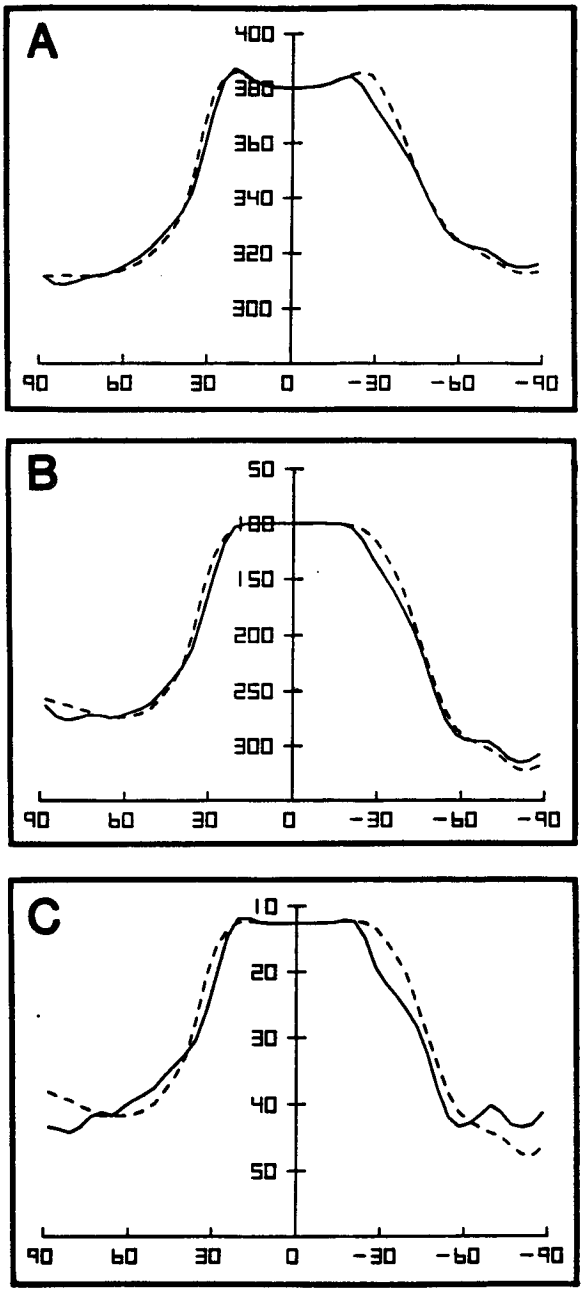

FIG. 2. Time and zonally averaged distributions on the tropopause for January 1979 of (a) potential temperature (K), (b) pressure (mb), and (c) isentropic mass density (kg m^{-2} K^{-1}). Solid (dashed) contours denote values on the dynamical (thermal) tropopause.

The total cross-tropopause mass flux within a zonal ring for January 1979 is defined as

$$\langle F(\rho) \rangle = \int \int_{\phi}^{\phi+\Delta\phi} \int_{0}^{2\pi} F(\rho) a^2 \cos\phi d\lambda d\phi dt, \quad (7)$$

where a is the earth's radius, t is time, λ is longitude, and ϕ is latitude. The time integral spans the 58 12-h analyses from 0000 UTC 2 January through 1200 UTC 30 January 1979, and $\Delta\phi = 3.75°$. Corresponding integrals for the various contributions to $F(\rho)$ in (1) are also evaluated. The results are shown graphically for the thermal tropopause in Fig. 3a and for the dynamical tropopause in Fig. 3b (the tendency term is not shown owing to its small *local* contribution). In all subsequent figures, a mass flux into the stratosphere (troposphere) is assigned a positive (negative) value.

The two estimates of the zonally integrated cross-tropopause mass flux (bold, solid contours) are qualitatively similar in the sense that they possess the same sign distributions within broad latitude bands (see Table 1). Substantial local differences, however, occur in the magnitudes of ST exchange, despite the close agreement between the meridional structures of the two time and zonally averaged tropopause surfaces (see Fig. 2). The two estimates also differ in the sign of the ST exchange at some latitudes (e.g., near 75°N, 20°N, and 60°S). The local differences largely reflect differences in the diagnosed adiabatic exchange along isentropes intersecting the tropopause (thin, solid contours). Differences in the diabatic mass flux (dashed contours) are also large in the 20°–50° latitude bands of both hemispheres with the flux across the dynamical tropopause being stronger.

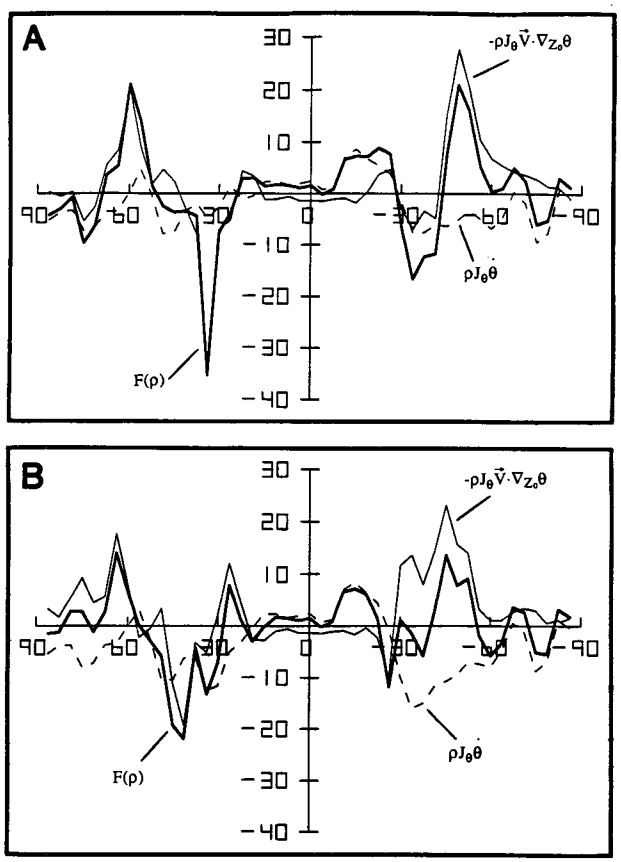

FIG. 3. Time and zonal integrals of the cross-tropopause mass flux (10^{15} kg) during January 1979 for the (a) thermal tropopause and (b) dynamical tropopause. Positive values indicate mass flux from the troposphere into the stratosphere. Bold, solid contours denote total mass flux; thin, solid contours denote the quasi-horizontal adiabatic mass flux; dashed contours denote the diabatic mass flux.

TABLE 1. Total mass exchange (10^{15} kg per month) across the tropopause within latitude bands.[a,b]

Latitude	$F(\rho)_{\text{dynamical}}$	$F(\rho)_{\text{thermal}}$
90°N–70°N	2	−24
70°N–50°N	20	45
50°N–25°N	−64	−60
25°N–25°S	26	44
25°S–40°S	−18	−28
40°S–70°S	26	45
70°S–90°S	−3	−5
90°N–90°S	−11	18
Stratospheric mass change[c]	4	1

[a] Positive values denote exchange from troposphere to stratosphere.
[b] The latitude bands were chosen from the zero crossings of $F(\rho)$ in Fig. 3.
[c] Derived from the globally integrated tropopause pressure tendency during January 1979.

While there is considerable uncertainty in the estimates of ST exchange as suggested above, several large-scale features are common in both analyses. The total mass flux is into the stratosphere between approximately 25°N and 25°S, where the diabatic mass transport is the primary contributor. This upward flux is strongest at the Southern Hemisphere (SH) tropical tropopause, consistent with the latitude of strongest atmospheric heating during January (see Schaack et al. 1990).

Stratospheric–tropospheric mass exchange in middle and subpolar latitudes is dominated locally by adiabatic transport along isentropes intersecting the tropopause. The mass flux is into the troposphere in the bands 25°–50°N and 25°–40°S. Locally, this exchange is considerably more intense when diagnosed with respect to the thermal tropopause (Fig. 3a) than the dynamical tropopause (Fig. 3b). The total exchange integrated over the aforementioned latitude bands, however, is relatively similar (see Table 1). The strong extrusion of stratospheric air at low latitudes of the extratropics supports the premise, based on case studies cited in the Introduction, that the climatological influence of baroclinic disturbances is to transport mass into the troposphere. We show in section 4 that the largest outflow of mass from the stratosphere indeed occurs near the cyclogenetic regions located at the western edges of the North Pacific and Atlantic storm tracks.

An important result is that the mean outflow of stratospheric mass in the midlatitude bands of 25°–50°N and 25°–40°S significantly exceeds the tropical inflow. Table 1 shows that between 80×10^5 and 90×10^{15} kg of mass enters the troposphere in these re-

gions. Less than half as much mass enters the stratosphere across the tropical tropopause. This is contrary to the notion that the ingress of tropical tropospheric air is balanced by the egress of midlatitude stratospheric air (WMO 1986). Instead, substantial mass flux into the stratosphere occurs between 50°–70°N and 40°–70°S. Perhaps somewhat surprising is the result that the intrusion of tropospheric mass in each of these latitude bands is as intense as that across the tropical tropopause. The mechanisms are different, with adiabatic exchange dominating in the extratropics and diabatic transport dominating in the tropics.

Additional insight into the mechanism of quasi-horizontal adiabatic exchange is provided through the following statistical decomposition. For a time and zonal integral, term (c) of (1) may be expressed as

$$-[\overline{\rho J_\theta \mathbf{V}\cdot\nabla_{Z_0}\theta}] = -\frac{1}{a}[\overline{\rho J_\theta v}]\frac{\partial[\bar{\theta}]}{\partial\phi_{Z_0}} - [\overline{(\rho J_\theta \mathbf{V})^*\cdot(\nabla_{Z_0}\theta)^*}] - [\overline{(\rho J_\theta \mathbf{V})'\cdot(\nabla_{Z_0}\theta)'}], \quad (8)$$

where brackets denote zonal integrals, overbars denote time integrals, and asterisks and primes denote zonal and time departures, respectively. The right-side terms in (8) represent contributions associated with the mean meridional circulation (MMC), stationary eddies, and transients, respectively.

The net contribution of the MMC to $F(\rho)$ can be given by

$$\text{MMC} = -\frac{1}{a}[\overline{\rho J_\theta v}]\frac{\partial[\bar{\theta}]}{\partial\phi_{Z_0}} + [\overline{\rho J_\theta \dot{\theta}}]. \quad (9)$$

Figure 4 illustrates the relative contributions of the statistical components in (8) and (9) to $\langle F(\rho)\rangle$ for both thermally [panel (a)] and dynamically [panel (b)] derived tropopause surfaces. Not surprisingly, the MMC (thin, solid contour) determines the cross-tropopause mass flux (bold, solid contour) in the tropics. In subpolar latitudes, however, the cross-tropopause mass flux is determined primarily by the stationary eddy and transient transports (dashed contour; includes also the small contribution by temporal fluctuations in the tropopause potential temperature). The contribution to the exchange by the quasi-horizontal branch of the MMC [first right-side term in (9)] is negligible in subpolar latitudes (not shown). This is consistent with the condition that the time- and zonal-mean meridional gradient of potential temperature becomes quite small poleward of 50° latitude (see Fig. 2b). Indeed, except in the vicinity of the time- and zonal-mean "tropopause break" that separates tropical and polar air, the contribution to $\langle F(\rho)\rangle$ by the MMC is determined primarily by its diabatic ($\rho J_\theta \dot{\theta}$) branch (not shown).

As a test of the robustness of the cross-tropopause mass flux diagnostics, we examine the time and area integrals of the ST exchange over the NH polar cap from 90°N to any latitude ϕ

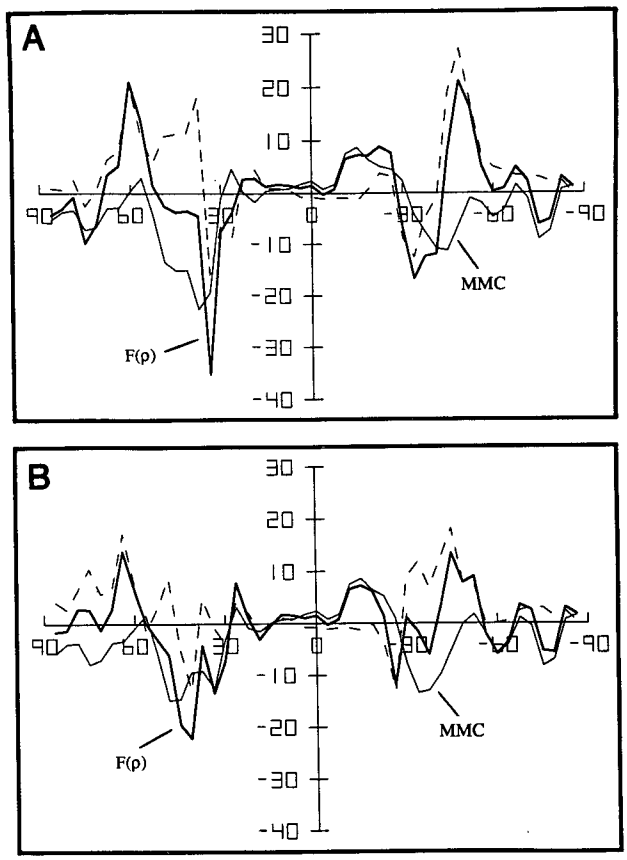

FIG. 4. Time and zonal integrals of the cross-tropopause mass flux (10^{15} kg) during January 1979 for the (a) thermal tropopause and (b) dynamical tropopause. Positive values indicate mass flux from the troposphere into the stratosphere. Bold, solid contours denote total mass flux; thin, solid contours denote the contribution by the mean meridional circulation (MMC); dashed contours denote the contribution by stationary eddy and transient transports plus the mass flux associated with temporal fluctuations of the tropopause potential temperature.

$$\{F(\rho)\} = \int\int_{\phi}^{\pi/2}\int_{0}^{2\pi} F(\rho)a^2\cos\phi\, d\lambda\, d\phi\, dt. \quad (10)$$

The curves in Fig. 5 illustrate the cumulative contribution of exchange processes along the path of integration beginning at the North Pole and ending at the South Pole. When integrated over the entire earth ($\phi = -\pi/2$), $\{F(\rho)\}$ measures the global stratospheric mass budget (see Wei 1987). A balanced mass budget requires that net global cross-tropopause mass flux be equal to the corresponding global integral of the tropopause pressure tendency over the month. As in Fig. 3, Figs. 5a and 5b reveal the exchange across the thermal and dynamical tropopause, respectively.

The global integral of $F(\rho)$ during January 1979 (bold, solid contour) is a small residual of adiabatic exchange into the stratosphere (thin, sold contour) and diabatic exchange into the troposphere (thin, dashed contour). Although small locally, the mass flux asso-

ciated with temporal fluctuations of tropopause potential temperature (bold, dashed contour) is also seen to be an important effect in the global budget due to the predominance of one sign globally.

The aforementioned interpretation of the global budget is relatively insensitive to tropopause definition. Indeed, it is encouraging that the meridional variation of the integrated ST mass exchange across progressively larger polar caps (from left to right in Fig. 5) agree qualitatively for the two surfaces. Large differences, however, in the magnitudes of the corresponding terms in Figs. 5a and 5b are apparent, especially in the vicinity of 30°S. The globally integrated cross-tropopause mass-flux estimates differ, with 18×10^{15} kg exchanged into the stratosphere across the thermal tropopause and 11×10^{15} kg exchanged into the troposphere across the dynamical tropopause. These values are to be compared with a net troposphere-to-stratosphere exchange of 1×10^{15} and 4×10^{15} kg, respectively, estimated from the tropopause pressure tendency over the month (see Table 1). Considering the uncertainties in calculating the ST exchange, with the global integral of $F(\rho)$ being determined by the residual of large terms of nearly equal magnitude and opposite sign, the agreement is encouraging. Substantial uncertainty in the global integral, however, is apparent.

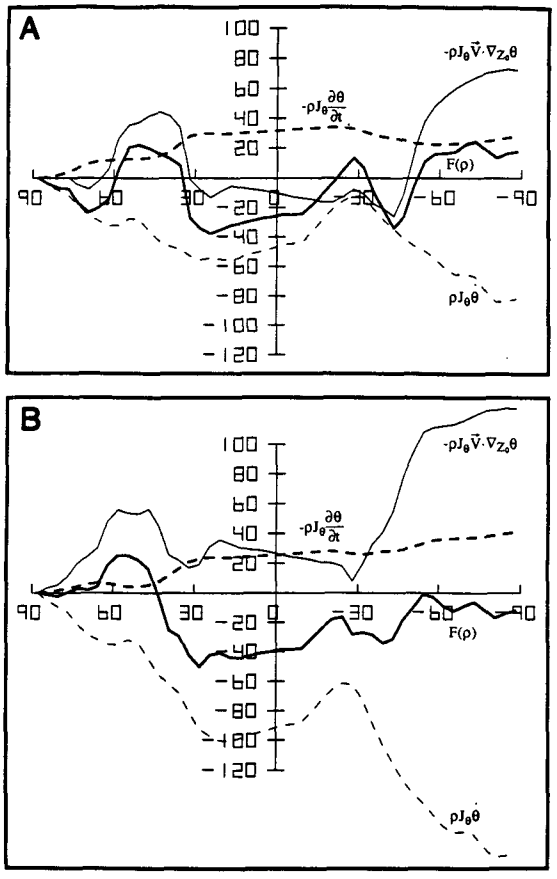

FIG. 5. Time and area integrals of the cross-tropopause mass flux (10^{15} kg) over the Northern Hemisphere polar cap from 90°N to any latitude ϕ during January 1979 for the (a) thermal tropopause and (b) dynamical tropopause. Positive values indicate mass flux from the troposphere into the stratosphere. Bold, solid contours denote the total mass flux; thin, solid contours denote the quasi-horizontal adiabatic mass flux; bold, dashed contours denote the mass flux associated with temporal fluctuations of the tropopause potential temperature; thin, dashed contours denote the diabatic mass flux.

4. The regional distribution of ST exchange

Pressure topographies on both the thermally (Fig. 6a) and dynamically (Fig. 6b) defined tropopause surfaces for January 1979 resemble the upper-level geopotential-height pattern (not shown). High tropopause pressures with values near 300 mb coincide with large-scale troughs over central Europe, eastern Asia, and central Canada. Comparatively low tropopause pressures are found in the downstream ridges over the western Soviet Union, the eastern Pacific, and the central Atlantic.

The largest regional differences between the two tropopause pressure topographies (Fig. 6c) are concentrated narrowly along the latitudes of the subtropical jets. Thermally derived pressures are 20–40 mb lower in this band, indicative of a steeper tropopause slope as also revealed in the zonally averaged cross sections (Fig. 2).

The time-mean ST exchange for January 1979 is shown in Figs. 7a and 7b for the thermal and dynamical tropopause surfaces, respectively. A prominent feature in the tropics is the strong flux into the stratosphere centered near New Guinea. This feature coincides with the region of maximum upper-level heating during January 1979 (see Schaack et al. 1990) associated with deep moist convection within the Australasian monsoon. These results support Newell and Gould-Stewart's (1981) hypothesis of a tropical stratospheric fountain in which the flux of tropospheric air into the stratosphere is confined to a limited area. The results in Fig. 7 indicate that other regions of the tropics including the Indian Ocean intertropical convergence zone and the South Pacific convergence zone are also characterized by a mass inflow to the stratosphere, although with reduced intensity.

A strong localization of the cross-tropopause mass flux also occurs in midlatitudes, although the details differ considerably between the two analyses. In general, the intensity of the exchange with respect to the thermal tropopause is considerably stronger than with respect to the dynamical tropopause. Perhaps the most prominent feature common to both is the intense outflow from the stratosphere over eastern China and the eastern United States. These centers lie within the base of the Asian and North American trough axes, and nearly overlay the major cyclogenetic regions observed during January 1979 (L. Keller 1988, personal communication). There is a suggestion that the mass flux into the

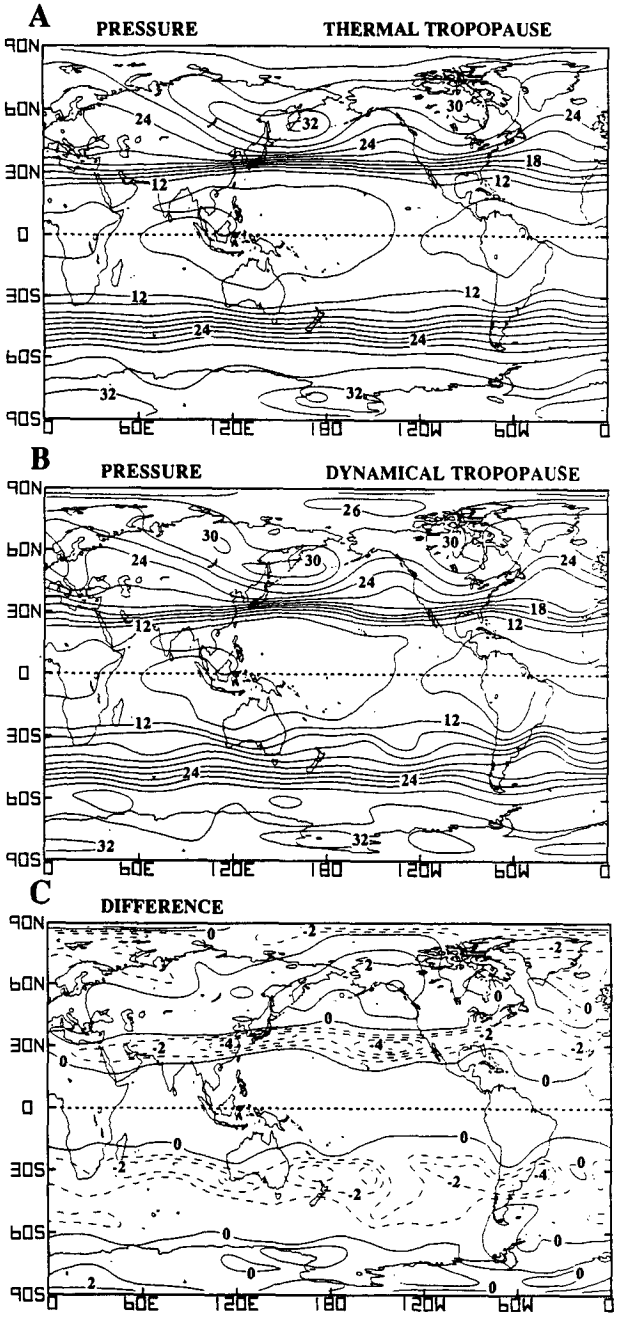

FIG. 6. Global analysis for January 1979 of pressure on the (a) thermal tropopause (10^1 mb), (b) dynamical tropopause (10^1 mb), and (c) the difference field (a) − (b) (10^1 mb).

troposphere over SH midlatitudes also coincides with stationary wave troughs. Four to five centers of strong exchange are evident between 30° and 40°S in Fig. 7a, which are in close proximity to individual trough axes of the observed wavenumber 5 circulation pattern during the GWE winter (Salby 1982; Trenberth 1984; Kalnay et al. 1986). The stratospheric mass outflow along the mean trough axes is due to both adiabatic mass transport and diabatic transport due to radiational cooling, both of which contribute to mean sinking motion at the tropopause (not shown).

A transport of mass to the stratosphere is generally found downstream and poleward of the midlatitude outflow regions. This pattern is particularly well defined over the northeastern Soviet Union, the North Pacific, western North America, and portions of the Southern Ocean. The inflow of mass to the stratosphere in these regions is primarily due to quasi-horizontal transport along isentropes that slope upward from the tropical low troposphere to the polar stratosphere (not shown). It is unlikely that individual air parcels follow such a simple ascending trajectory. The results in Fig. 7, however, imply that the time-mean effect of airmass migrations downstream of the stationary troughs is to transport mass of low-latitude origin poleward and upward across the high-latitude tropopause.

For the most part, the results in Fig. 7 indicate a preference for stratospheric mass outflow at low lati-

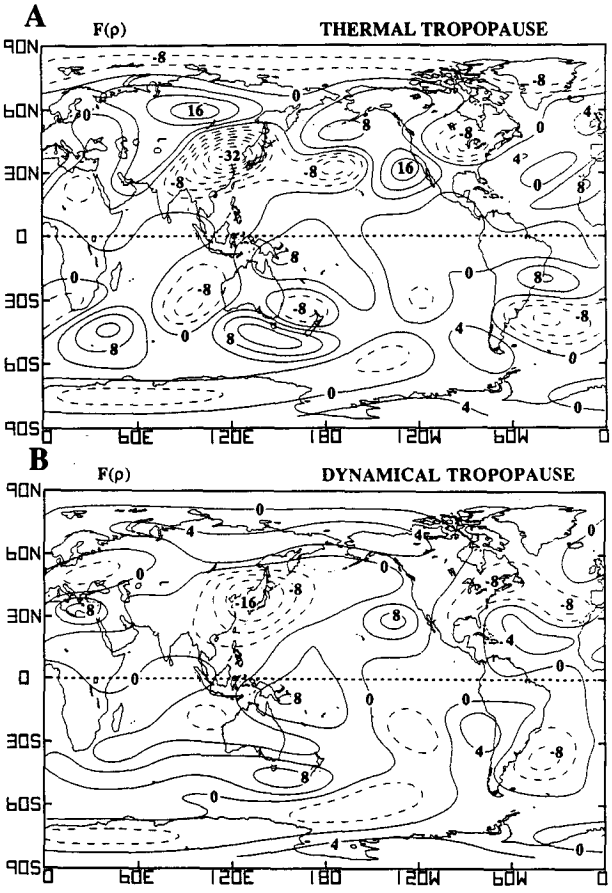

FIG. 7. Global analysis for January 1979 of the stratospheric–tropospheric mass exchange for the (a) thermal tropopause and (b) dynamical tropopause. Contour interval is 4×10^{-4} kg m^{-2} s^{-1}. Solid contours denote a time-mean mass flux from the troposphere into the stratosphere. Filtered to emphasize contributions from zonal wavelengths greater than 6000 km.

tudes of extratropics near quasi-stationary troughs, and a return mass flow to the stratosphere at high latitudes of extratropics near quasi-stationary ridges. These regional results are consistent with our statistical analysis of the zonally integrated quasi-horizontal exchange process that revealed the important contribution of stationary eddies and transients in middle and subpolar latitudes. It would thus appear that the regional pattern of time-mean ST exchange in extratropics is interpretable within the framework of conceptual models on the airflow in baroclinic disturbances. For example, Palmen and Newton's (1969) composite of the three-dimensional air motion in cyclones includes sinking trajectories to the rear of a surface wave, typically associated with equatorward movement of polar air along the axis of an upper-level trough. Ascending trajectories occur over the warm sector in association with the poleward movement of tropical air beneath a downstream upper-level ridge. We have verified that the regions of strong stratospheric mass outflow in Fig. 7 experience mean subsidence at the tropopause, while regions of mass inflow to the stratosphere tend to be accompanied by ascent (not shown). The correlation between subsidence at the tropopause, adiabatic exchange and stratospheric extrusion for the general circulation as shown here compliments Danielsen's (1964) model of the synoptic-scale ST exchange derived from Project Springfield. His results and several subsequent investigations, however, failed to address the nature of mass flow in the warm ascending branch. Our results suggest that the subpolar ingress to the stratosphere occurs along a "conveyor" of large-scale slantwise convection. This supports Johnson's (1979) hypothesis that quasi-horizontal isentropic flow in amplifying baroclinic disturbances may be an effective mechanism for the return transport of mass to the stratosphere.

5. Concluding remarks

Our investigation of the global and time-mean mass transport across the tropopause has been motivated by several considerations. Foremost is the paucity of planetary-scale studies of ST exchange for extended time periods. Reiter's (1975) precedent study, which serves as the most definitive global analysis to date, attempts to incorporate results from regional case studies into a large-scale framework. Such an effort necessarily requires approximations. Perhaps the most severe involves the extratropical exchange. Case-study results are consistent in revealing outflow of stratospheric air over the polar front region between 30° and 50°N, thus arguing for the utility of a cyclone index for estimating the climatological flux in midlatitudes. Indeed, our zonally integrated results in midlatitudes are consistent with the inferences based on such a cyclone index. It is also assumed in Reiter (1975), however, that an eddy-induced mass outflow of similar intensity occurs over subpolar latitudes. This latter assumption is not corroborated by our results. The latitude bands of 50°–70°N and 40°–70°S are found to be principal regions in the global atmosphere where tropospheric mass *enters* the stratosphere during January 1979. The exchange appears intimately related to stationary eddy and transient transports.

Our mass-transport diagnostics revealing inflow to the stratosphere at subpolar latitudes appear to be consistent with independent analyses of trace atmospheric constituents. Several studies using satellite and research aircraft data have confirmed high water vapor contents, indicative of tropospheric values, in the low stratosphere over the subpolar latitudes. Monthly and zonal-mean analyses using Limb Infrared Monitor of the Stratosphere (LIMS) data during 1979 show maxima in water vapor content at high latitudes near 100 mb (WMO 1986; see Figs. 9.19 and 9.20). Confirmation of the LIMS data is provided by aircraft measurements for shorter periods at two high-latitude locations near Punta Arenas (53°S) and Stavanger (59°N) (Kelly et al. 1990). The authors comment that the abundance of water vapor near the tropopause at high latitudes is "consistent with non-tropical entry of some air." Kelly et al. (1991) suggest that "sloping convection" within cyclone circulations can be an effective agent for poleward and upward transport of water vapor across the high-latitude tropopause.

Additionally, the regions of mass inflow across the subpolar tropopause should be characterized by ozone minima in the low stratosphere. High-latitude Northern Hemisphere ozonesonde ascents have, in fact, shown a highly laminated structure in the lower stratosphere consistent with exchange from the troposphere to the stratosphere. Dobson (1973) found a statistical preference for ozone minima to occur at high latitudes near 15 km (roughly 100 mb). These minima were most frequent during winter–spring when they appeared on over 50% of the days. Based on analysis of several North American ozonesonde ascents, Dobson argues that the high-latitude minima near 15 km originate from a mass flux into the stratosphere in middle latitudes. Analogous to the mechanism suggested by Kelly et al. (1991), the ozone-poor air presumably travels poleward in advance of large-scale cyclonic disturbances.

The outcome of the above intercomparison, while by no means conclusive, nonetheless appears to provide confirmation of our principal result concerning mass flux into the stratosphere at the subpolar latitudes. The qualitative picture emerging herein may have significant implications for stratospheric chemistry, the upper-tropospheric water vapor budget, and greenhouse warming. An additional issue involves the environmental impact of aircraft exhaust emissions. Robinson (1980) proposed a stratospheric–tropospheric mass-exchange hypothesis based on analysis of minor atmospheric constituents. His hypothesis closely followed Reiter's model, including transport into the strato-

sphere over the tropics and return flow to the troposphere near the midlatitude "tropopause gap." Inferences of the high-latitude exchange were not possible, however, owing to the lack of reliable observations. Our results of the high-latitude ST mass exchange together with the aforementioned LIMS and aircraft data reveal potentially large time-mean mass inflow to the stratosphere poleward of the midlatitude tropopause gap. As such, aircraft emissions may not have as large a tropospheric lifetime as initially presumed in Robinson's study.

It would be premature to argue that the picture of the wintertime extratropical ST exchange derived from the current analysis supersedes previous ones. Indeed, considerable quantitative uncertainty exists in our analysis of both the regional and zonally integrated ST exchange as evidenced by the differences in estimates for the dynamically and thermally defined tropopause surfaces. Additionally, analysis of ST exchange for a single month may not be representative of the climatological exchange. Extension of the current study to additional months and years is clearly required.

A second motivation for this investigation is that the chemistry of the troposphere and stratosphere is known to depend sensitively on the exchange of mass and trace species across the tropopause (see WMO 1986). Diagnosing global ST mass exchange is thus a useful first step to improving our understanding of the various chemical processes. We are particularly intrigued by the large influx of mass to the stratosphere at high latitudes and the possible implications for polar stratospheric chemistry. Yet, knowledge of the mass exchange alone is only of limited value. The transport of photochemically active trace gases including CFCs, CH_4, CO_2, etc., requires knowledge of their correlation with the mass circulation. At this time, a lack of three-dimensional datasets for these gases precludes such observational studies. An interim approach may be to use synthetic datasets of gaseous distributions produced by a general circulation model (GCM). Allam and Tuck (1984) used a three-dimensional GCM to diagnose the cross-tropopause flux of water vapor, an analysis that is difficult with observed data owing to the poor quality of upper-level water vapor measurements. Three-dimensional GCMs that include physical and chemical models for trace species are still in their infancy, although the results in Grose et al. (1987) and Rood et al. (1990) are encouraging.

Acknowledgments. A portion of this research was performed while the first author was at the University of Wisconsin. Discussions with Dr. Adrian Tuck were very helpful, especially with respect to relating our results to previous studies of upper-level water vapor. We appreciate the comments of two anonymous reviewers that helped improve the paper's focus. We gratefully acknowledge the technical assistance of Judy Mohr and Cindy Karls in preparing the manuscript. This research was supported by NASA Grant NAG5-81.

REFERENCES

Allam, R. J., and A. F. Tuck, 1984: Transport of water vapor in a stratosphere–troposphere general circulation model. I: Fluxes. *Quart. J. Roy. Meteor. Soc.*, **110,** 321–356.

Danielsen, E. F., 1959: The laminar structure of the tropopause and its relation to the concept of the tropopause. *Arch. Meteor. Geophys. Bioklim.*, **BII,** 293–332.

——, 1964: Project Springfield Rep., Washington, D.C., Defense Atomic Support Agency Rep., DASA 1517, 97 pp.

——, 1968: Stratospheric–tropospheric exchange based on radioactivity, ozone and potential vorticity. *J. Atmos. Sci.*, **25,** 502–518.

——, 1984: Meteorological context for global tropospheric experiments' instruments tests. *EOS Trans.*, Amer. Geophys. Union, **65,** 834.

——, and R. S. Hipskind, 1980: Stratospheric–tropospheric exchange at polar latitudes in summer. *J. Geophys. Res.*, **85,** 393–400.

Defant, F., and H. Taba, 1957: The three-fold structure of the atmosphere and characteristics of the tropopause. *Tellus,* **9,** 259–274.

Dobson, G. M. B., 1973: The laminated structure of the ozone in the atmosphere. *Quart. J. Roy. Meteor. Soc.*, **99,** 599–607.

Grose, W. L., J. E. Nealy, R. E. Turner, and W. T. Blachsheu, 1987: Modeling the transport of chemically active constituents in the stratosphere. *Transport Processes in the Middle Atmosphere,* G. Visconti and R. R. Garcia, Eds., Reidel, 215–228.

Hoerling, M. P., T. K. Schaack, and A. J. Lenzen, 1991: Global objective tropopause analysis. *Mon. Wea. Rev.*, **119,** 1816–1831.

Johnson, D. R., 1979: Systematic stratospheric–tropospheric exchange through quasi-horizontal transport processes within active baroclinic waves. *Proc. Symp. on the Long-Range Transport of Pollutants and its Relation to General Circulation Including Stratospheric-Tropospheric Exchange Processes,* Sofia, Bulgaria, World Meteorological Organization, 401–408.

——, 1980: A generalized transport equation for use with meteorological coordinate systems. *Mon. Wea. Rev.*, **108,** 733–745.

Kalnay, E., K. C. Mo, and J. Paegle, 1986: Large-amplitude short-scale stationary Rossby wave in the Southern Hemisphere: Observations and mechanistic experiments to determine their origin. *J. Atmos. Sci.*, **43,** 252–275.

Kelly, K. K., A. F. Tuck, L. E. Heidt, M. Loewenstein, J. R. Podolske, S. E. Strahan, and J. F. Vedder, 1990: A comparison of ER-2 measurements of stratospheric water vapor between the 1987 Antarctic and 1989 Arctic Airborne Missions. *Geophys. Res. Lett.*, **17,** 465–468.

——, ——, and T. Davies, 1991: Wintertime asymmetry of upper tropospheric water between the Northern and Southern hemispheres. *Nature,* **353,** 244–247.

Krishnamurti, T. N., 1961: The subtropical jet stream of winter. *J. Meteor.*, **18,** 172–191.

Kritz, M. A., S. W. Rosner, E. F. Danielsen, and H. B. Selkirk, 1991: Air mass origins and troposphere-to-stratosphere exchange associated with mid-latitude cyclogenesis and tropopause folding inferred from ^{7}Be measurements. *J. Geophys. Res.*, **96,** 17 405–17 414.

Mahlman, J. D., 1964: Relation of stratospheric–tropospheric exchange mechanisms to surface radioactivity peaks. *Arch. Meteor. Geophys. Bioklim.*, **15,** 1–25.

Newell, R. E., and S. Gould-Stewart, 1981: A stratospheric fountain? *J. Atmos. Sci.*, **38,** 2789–2796.

Palmen, E., and C. W. Newton, 1969: *Atmospheric Circulation Systems.* Academic Press, 603 pp.

Reed, R. J., 1955: A study of a characteristic type of upper level frontogenesis. *J. Meteor.*, **12,** 226–237.

——, and E. F. Danielsen, 1959: Fronts in the vicinity of the tropopause. *Arch. Meteor. Geophys. Bioklim.*, **11,** 1–17.

Reiter, E. R., 1975: Stratospheric-tropospheric exchange processes. *Rev. Geophys. Space Phys.*, **13,** 459–474.

——, M. E. Glasser, and J. D. Mahlman, 1969: The role of the tropopause in stratospheric-tropospheric exchange processes. *Pure Appl. Geophys.*, **12,** 183–221.

Robinson, G. D., 1980: The transport of minor atmospheric constituents between troposphere and stratosphere. *Quart. J. Roy. Meteor. Soc.*, **106,** 227–253.

Rood, R. B., J. A. Kaye, A. R. Douglas, D. J. Allen, S. Steenrod, and E. M. Larson, 1990: Wintertime nitric acid chemistry: Implications from 3-D model calculations. *J. Atmos. Sci.*, **47,** 2696–2709.

Salby, M. L., 1982: A ubiquitous wavenumber-5 anomaly in the Southern Hemisphere during FGGE. *Mon. Wea. Rev.*, **110,** 1712–1720.

Schaack, T. K., D. R. Johnson, and M.-Y. Wei, 1990: The three-dimensional distribution of atmospheric heating during the GWE. *Tellus*, **42A,** 305–327.

Shapiro, M. A., 1980: Turblent mixing within tropopause folds as a mechanism for the exchange of chemical constituents between the stratosphere and troposphere. *J. Atmos. Sci.*, **37,** 994–1004.

——, T. Hampel, and A. J. Kreuger, 1987: The arctic tropopause fold. *Mon. Wea. Rev.*, **115,** 444–454.

Staley, D. O., 1960: Evaluation of potential vorticity changes near the tropopause and the related vertical motions, vertical advections of vorticity, and transfer of radioactive debris from the stratosphere to the troposphere. *J. Meteor.*, **17,** 591–620.

——, 1962: On the mechanism of mass and radioactivity transport from stratosphere to troposphere. *J. Atmos. Sci.*, **19,** 450–467.

Trenberth, K. E., 1984: Interannual variability of the Southern Hemisphere circulation: Representativeness of the year of the Global Weather Experiment. *Mon. Wea. Rev.*, **112,** 108–123.

Wei, M.-Y., 1987: A new formulation of the exchange of mass and trace constituents between the stratosphere and troposphere. *J. Atmos. Sci.*, **44,** 3079–3086.

World Meteorological Organization, 1986: Atmospheric ozone 1985: Global ozone research and monitoring rep. WMO Rep. No. 16, 392 pp.